J. Physiol. (1982), **324**, *pp.* 507–533
With 13 *text-figures*
Printed in Great Britain

EFFECTS OF EXTRACELLULAR POTASSIUM ACCUMULATION AND SODIUM PUMP ACTIVATION ON AUTOMATIC CANINE PURKINJE FIBRES

BY RICHARD P. KLINE AND JOEL KUPERSMITH

From the Departments of Pharmacology and Medicine, Mount Sinai School of Medicine, C.U.N.Y., New York NY 10029, U.S.A.

(*Received 5 December 1980*)

SUMMARY

1. Double barrel potassium-sensitive micro-electrodes were used to measure fluctuations in extracellular potassium ion concentration in large automatic canine Purkinje fibres.

2. Slow accumulations of potassium were seen in the extracellular space during prolonged beating. Following cessation of prolonged beating, a depletion of extracellular potassium ions was noted.

3. The time course of these slow changes in extracellular potassium concentration were shown to be a function of the diffusion properties of the preparation, and the rate and degree of activation of the sodium pump.

4. Action potential duration and maximum diastolic potential were simultaneously monitored during and after these periods of rapid stimulation, using conventional intracellular micro-electrodes.

5. Initial depolarization and later hyperpolarization of the maximum diastolic potential appeared to occur as a direct result of changes in extracellular potassium concentration and level of pump activation induced by the sudden and prolonged alteration in stimulus rate.

6. Following prolonged stimulation, dramatic changes in the automatic beating rate were correlated with changes in extracellular potassium and pump rate, and their effects on the maximum diastolic potential and other parameters of the diastolic potential depolarization.

7. For some locations of the potassium-sensitive electrode tip, large fluctuations in extracellular potassium were seen during single beats. Alterations in action potential duration during abrupt rate changes appear to derive in part from modulation by these extracellular potassium concentration fluctuations altering net membrane currents. Slower shifts in action potential duration appear correlated to the degree of sodium pump activation.

INTRODUCTION

It has long been predicted that currents associated with cardiac activity carried sufficient numbers of ions to alter ionic concentrations on one or both sides of the

membrane (MacAllister & Noble, 1966). Due to the large ratio of the membrane area to the volume of the restricted extracellular space in most cardiac tissue types, particular attention has been given to the problem of extracellular K^+ accumulation (Baumgarten & Isenberg, 1977; Cohen, Daut & Noble, 1976; Attwell, Eisner & Cohen, 1979; Noble, 1976). The availability of rapid response time ion-sensitive electrodes for K^+ (Neher & Lux, 1973) and the low base line concentrations of extracellular K^+ have facilitated the study of this phenomenon directly (Kline & Morad, 1976; Kunze, 1977).

The characterization of the extracellular K^+ fluctuations during cardiac activity is particularly important in light of the recent dependence on the voltage-clamp technique for most of the detailed quantitative description of the ionic currents flowing during the cardiac action potential (Trautwein, 1973; MacAllister, Noble & Tsien, 1975). In particular, it is important to know whether the time dependence of any of the K^+ channels is due in some part to changes in extracellular K^+ concentration. Such extracellular changes in K^+ would give a distinct time dependence to the rectifier functions of the various K^+ selective channels (Attwell *et al.* 1979).

In previous studies with canine Purkinje fibres (Kline, Cohen, Falk & Kupersmith, 1980) two basic aspects of K^+ accumulation have been demonstrated. First, during each action potential there is net K^+ efflux which, during rapid beating, summates and induces a slow accumulation of base line extracellular K^+ on which the beat-to-beat changes are superimposed. These results are similar to those in frog ventricle (Kline & Morad, 1976). Secondly, sustained depletions of extracellular K^+ are seen following rapid drive. This depletion has been attributed to activation of an Na–K pump (Kunze, 1977). Measureable outward currents are associated with this putative pump activation (Gadsby & Cranefield, 1979*a*; Eisner & Lederer, 1979; Kline *et al.* 1980; Cohen, Falk & Kline, 1981), and both extracellular K^+ accumulation and the pump-related measureable outward currents have been shown to affect action potential duration and automaticity in several cardiac tissue types (Vassalle, 1970; Gadsby & Cranefield, 1979*b*; Spear, Kronhaus, Moore & Kline, 1979; Kline *et al.* 1980).

It has been suggested that maximum diastolic potential (m.d.p.) in automatic Purkinje fibres is altered by fluctuations in extracellular K^+ concentration ($[K]_o$). Depolarization of m.d.p. during rapid overdrive stimulation has been attributed to extracellular K^+ accumulation (Vassalle, 1977; Browning, Tiedman, Stagg, Benditt, Scheinman & Strauss, 1979). Interventions which alter the reversal potential of the pacemaker current during voltage-clamp experiments have also been interpreted as reflecting changes in $[K]_o$ (Cohen *et al.* 1976; Cohen, Eisner & Noble, 1978).

In ventricular muscle, rapid stimulation leads to accumulation of extracellular K^+ and membrane depolarization (Kline & Morad, 1978). Hyperpolarization, which might be attributed to the effects of electrogenic Na–K pump activation, is not observed during stimulation. By contrast, in non-automatic Purkinje fibres, rapid stimulation induces extracellular K^+ accumulation (Kline *et al.* 1980) and membrane hyperpolarization (Vassalle, 1977). No depolarization is observed. In automatic Purkinje fibres, depolarization followed by hyperpolarization is observed in response to rapid stimulation (Browning *et al.* 1979). Thus, it appears that different tissues, under different experimental conditions, are variably susceptible to the effects of extracellular K^+ accumulation *per se* (which shifts the K^+ equilibrium potential in

a positive direction) and to the effects of electrogenic Na–K pump activity (a predominantly hyperpolarizing effect).

This study attempts to measure and compare simultaneously in large canine Purkinje fibres the changes in m.d.p. and $[K]_o$ during and after rapid beating, and in automatic diastolic interval after rapid beating. Additional parameters of the diastolic membrane depolarization are also considered during this post-drive period when the automatic rate is dramatically changing.

The response of action potential duration (a.p.d.) to changes in $[K]_o$ (Weidmann, 1956) and pump activity (Gadsby & Cranefield, 1979*b*) has been described. Carmeliet (1955) further proposed that an ion accumulating extracellularly during one beat could act to shorten a subsequent beat during sudden changes in diastolic interval. Such beat-to-beat fluctuations in $[K]_o$ have been shown to occur in frog ventricle (Kline & Morad, 1978) and appear to behave in the manner predicted by Carmeliet. A second aim of this study is to determine whether these same rate interventions which affect m.d.p. may also influence a.p.d.

A preliminary report of this work has been presented in abstract form (Kline & Kupersmith, 1980).

METHODS

The experimental methods are similar in most respects to those employed by Kline *et al.* 1980. Large free running canine Purkinje fibres were removed from the left or right ventricle of mongrel dogs and dissected in oxygenated Tyrodes solution with the aid of a dissecting microscope.

Tyrodes solution contained the following ionic constituents: 4 mM-KCl; 137 mM-NaCl; 1·8 mM-$CaCl_2$; 12 mM-$NaHCO_3$; 1·8 mM-NaH_2PO_4; 0·5 mM-$MgCl_2$ and 5·5 mM-dextrose. pH was adjusted to between 7·3 and 7·4. Temperature was maintained constant at 35 °C by superfusing solution at a fixed rate with a Sage pump (375A) through a coil whose outer reservoir was perfused with heated water from a Lauda pump (K2/R). Temperature was monitored by a Yellow Springs microprobe thermistor attached to a 73ATA meter unit. The solution was oxygenated with a 95 % O_2–5 % CO_2 gas mixture.

Conventional micro-electrodes (4–8 MΩ resistance) were inserted into the input probe of a W-P instruments model M707 micro-electrode amplifier. Double barrel K^+ ion-sensitive micro-electrodes were fabricated using standard techniques (Kline & Morad, 1978). The two barrels were attached by means of Ag–AgCl wires to the head stages of a dual input specially designed differential amplifier (Bloom Associates) which allowed for gain adjustments to be made on both barrels assuring common mode rejection of 0·1 % for test voltage pulses. During the course of an experiment, 100 mV test pulses 10 sec long were applied between the bath and ground (while the K^+ electrode was in the tissue). It was required that the response on the difference trace be less than 50 μV in order to proceed with the experiment.

Adjustments could be made to compensate for the slower response time of the ion-sensitive barrel by slowing the response time of the faster reference barrel with a variable active filter while at the same time enhancing the response time of the slower ion-sensitive barrel with capacitive compensation (Kronhaus, Spear, Kline & Moore, 1978). It should be noted that both barrels detect potential, but superimposed on the ion-sensitive barrel output is an additional electrical potential which reflects the changes in local K^+ activity at the electrode tip. Thus a differential mode is used to measure K^+ activity. The response time of the electrodes for such measurements is about 20 msec (Neher & Lux, 1973). Calibration procedures are as described in Kline & Morad (1978), and Kline (1975).

Using the experimental procedures described, fibres were often seen to be beating automatically at slow rates. Naturally beating fibres could be overdriven using a stimulator attached to two platinum wires brought near to one end of the preparation. Shorter unbranched fibres were used whenever possible.

Membrane potential (V_m), and plots of m.d.p. and $[K]_o$ were digitized either by hand or by using

a Textronic magnetic tablet. Exponential fitting was accomplished using a PDP 10 time sharing facility (Prophet 52; software developed by Bolt, Beranek and Newman; Cambridge, MA) and the 'Expfit' subroutine (see Prophet Public Procedures).

Electrical alternans was induced by suddenly changing the stimulator frequency from a slow equilibrated rate to a rapid rate for a short period of time. The effects of timed extrasystolic (S2) beats applied during periods of prolonged equilibrated beating (S1 beats) at a slower rate were also studied. The S2 beats were inserted with fixed intervals of delay in most cases during the diastolic period of the S1 beats. S2 beats were electronically inserted every sixth beat.

Careful positioning of the K^+ electrode is important in performing and interpreting these studies (Kline *et al.* 1980). Determination of whether the K^+ electrode tips are intracellular or extracellular can be achieved in two ways: first the reference barrel of the double barrel K^+ ion-sensitive micro-electrode measures potential as a standard micro-electrode. In fact, it was frequently possible to get stable intracellular punctures with the double barrel K^+ electrode. The reference barrel at these times measured normal resting potential. Secondly, on the differential output, the high levels of intracellular K^+ activity were reflected (Miura, Hoffman & Rosen, 1977; Lee & Fozzard, 1975).

If the electrode was pushed through the cell, or pulled back, there was a rapid decline in the output of the reference barrel and the measured K^+ activity levels receded to approximately those of the bathing solutions (Tyrodes). Beat-to-beat $[K]_o$ changes were only seen when the electrode tip remained in the extracellular spaces. As soon as normal transmembrane resting potentials were seen on the reference barrel, beat-to-beat fluctuations on the differential trace disappeared. At the same time normal intracellular action potential traces were seen on both barrels monitored individually.

Often the electrode was dislodged from the intercellular spaces after many minutes of rapid beating. When this occurred, the beat-to-beat changes in $[K]_o$ appeared smaller. Eventually, if the electrode was withdrawn further, no beat-to-beat changes were observed, and only an apparent average 'envelope' of accumulation was seen (Kline *et al.* 1980; Kline & Morad, 1978) upon sudden change in rate of stimulation. For the purposes of this study, we did not use punctures with V_0 changes greater than 12 mV, or punctures where the beat-to-beat $[K]_o$ changes were not stable for at least 10 min.

RESULTS

Effects of accumulation on a.p.d.

Accumulation of K^+ in the extracellular space of Purkinje fibres has been reported (Kline *et al.* 1980). For single beats, $[K]_o$ starts increasing during the early phases of the action potential plateau. Peak $[K]_o$ is detected later in the plateau, or in many cases at the start of the fast repolarization phase. During rapid repolarization $[K]_o$ falls rapidly.

Fig. 1 shows the membrane potential and $[K]_o$ recordings from a fibre stimulated (after a short period of quiescence) for four beats at a cycle length of 800 msec. After a pause of 3 sec, the fibre was again stimulated at the same cycle length. With both trains of stimuli, an alternans in a.p.d. was observed (a.p.d. to 90% repolarization indicated below each action potential in parenthesis). It can be seen in Fig. 1 that the two shortest a.p.d.s in the first train are the second and fourth beats. These two beats also have the two highest $[K]_o$ levels at their onset (at upstroke). The third a.p.d. in the first train is longer, and $[K]_o$ at the start of this beat has fallen below the value seen for beats two and four. The first beat, preceded by a period of quiescence, is the longest and the $[K]_o$ level is the lowest. The fifth beat which occurs after a pause is slightly shorter than the first beat; it occurs during the tail of $[K]_o$ decay from the first four beats. The sixth beat is shorter than the seventh beat. A higher $[K]_o$ level is recorded at its start.

The behaviour of the fluctuations in $[K]_o$ during a more complicated change in rate is shown in Fig. 2 for similar experimental conditions in another fibre. Both $[K]_o$ and

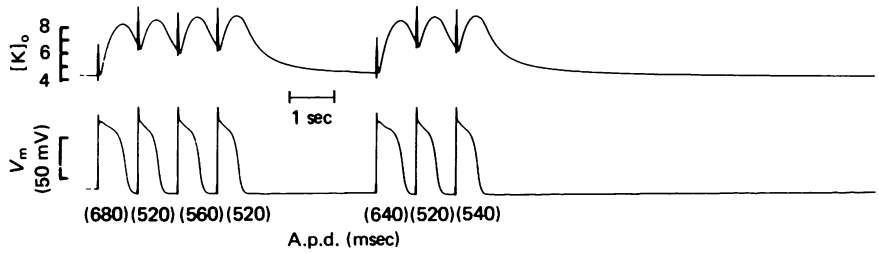

Fig. 1. The top trace shows extracellular $[K]_o$ fluctuations (K^+ electrode output displayed with millimolar calibration bars) during two short trains of rapid beats. Bottom traces are simultaneously-measured intracellular action potentials on a micro-electrode whose tip is positioned near that of the K^+ electrode. In parentheses beneath each action potential is the duration (a.p.d.) measured in milliseconds (to 90% repolarization). Note relation between a.p.d. and $[K]_o$ at the start of each beat. Temperature 37 °C.

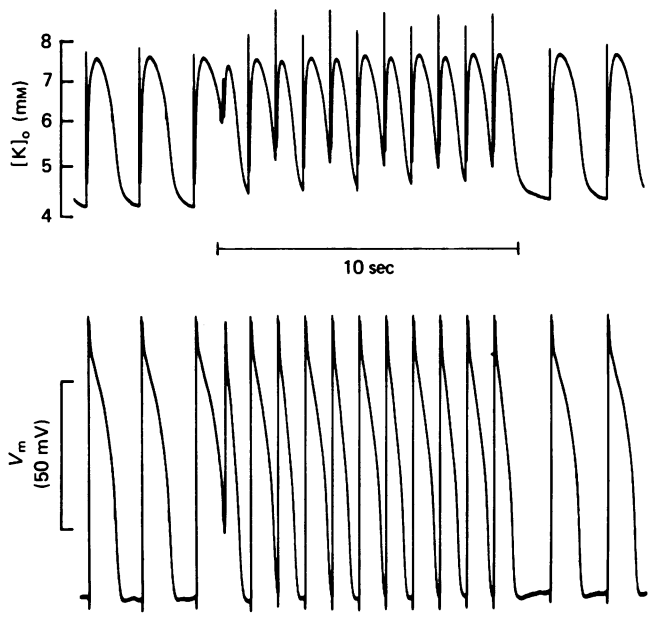

Fig. 2. The top trace represents the $[K]_o$ fluctuation (K^+ electrode output) during an alternans induced by an 11 sec interval of rapid beating (twelve beats at cycle lengths of 900 msec), with two beats at the previous control stimulus rate (cycle length 1700 msec) before and two beats after the alternans. The $[K]_o$ base line levels were elevated slowly during the initial control beats at cycle length 1700 msec. Following return to quiescence, $[K]_o$ decayed back to 4·0 mM (bath level) over a period of about 15 sec. These slow changes before and after the beats shown are omitted from the figure for clarity. The stimulus artifact was not completely eliminated in the differential mode. The bottom trace represents the potential recordings from an intracellular micro-electrode. Note the alternans in both a.p.d. and $[K]_o$ at the start of each beat. The fourth beat, which is the shortest, also has the highest $[K]_o$ levels at the onset. Except for this beat, the peaks of the $[K]_o$ fluctuations for each beat are approximately equal. Temperature 28 °C.

transmembrane potential recordings are shown during two control beats at a cycle length of 1700 msec after a period of quiescence. The stimulus frequency was then suddenly increased to 67/min (cycle length of 900 msec) for twelve beats. Two beats at the 1700 msec cycle length are then shown immediately following the train of rapid stimuli. Note the alternans in the a.p.d. of the action potentials during the rapid beats and the accompanying alternation in the pattern of the beat-to-beat $[K]_o$ changes.

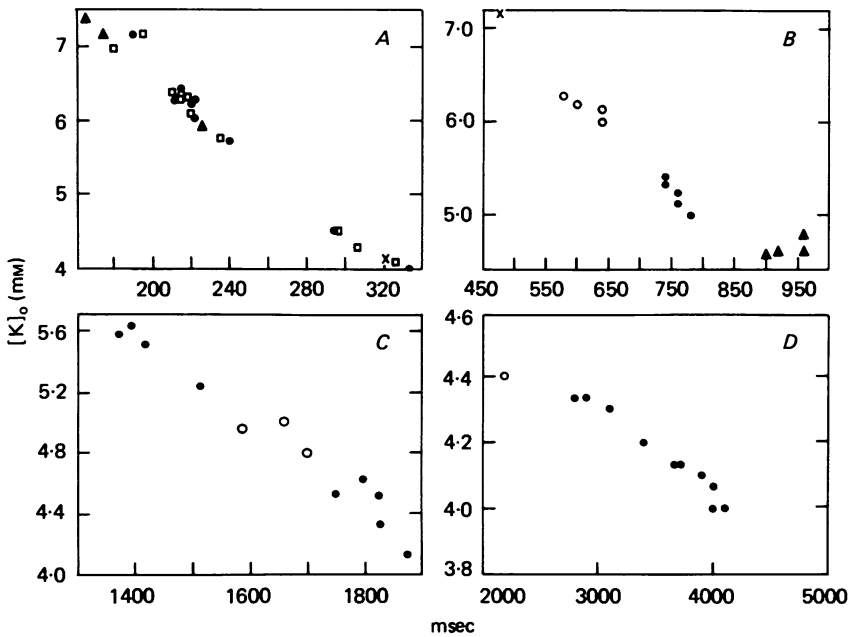

Fig. 3. Data is presented for various brief stimulus protocols in four different fibres at temperatures between 20 and 37 °C. Data for each action potential are plotted as a single point where the horizontal axis gives the a.p.d. (milliseconds to 50% repolarization) and the vertical axis represents the level of $[K]_o$ (millimolar) at the start of each beat. In all panels, initial levels of $[K]_o$ before beating were 4 mM. Different symbols are used for different action potentials in each panel to identify different portions of the stimulus protocols. This is described in detail in the text.

As the a.p.d.s of the alternating beats tended to converge slowly to an intermediate value, the values for $[K]_o$ at the start of each beat also converged to some intermediate value. The peaks of the cycle-dependent $[K]_o$ changes, however, appeared to remain approximately constant except for the fourth action potential which is dramatically shortened, and has a reduced upstroke.

Fig. 3 shows graphical representations of the relationship between a.p.d. and $[K]_o$ (at the start of each action potential) for experiments in four different fibres, at varying temperatures, with protocols similar to that described in Fig. 1 and 2.

In panel *A*, data showing a.p.d. versus $[K]_o$ at the start of each beat are plotted for three short trains (twelve beats each) of stimulated beats at stimulus interval 330 msec. Each train was started at various values of initial $[K]_o$, since the interval between trains was not sufficient for $[K]_o$ to completely decay. In addition, during one train, several beats at 270 msec cycle length were inserted at the end of the train;

and during a second train, a 680 msec cycle length beat was inserted during the train. (Each train is plotted with a separate symbol; temperature was 37 °C).

In panel *B*, similar data are shown for a single rapid train at a stimulus interval of 900 msec (28 °C; records for this train are shown and described in detail in Fig. 2 above). The points are clustered (each cluster is represented by a different symbol). The longest action potentials (symbols are filled triangles) were stimulated at a slower base line rate which itself had caused slight elevation of the $[K]_o$ levels. The single shortest point (symbol is an ' × ') is the first beat at the rapid rate. There are two further clusters (symbols are open and filled circles) due to an alteration between a long and a shorter a.p.d. at the fast rate.

After a quiescent period of several seconds (panel *C*), the fibre was stimulated for nine beats with a varying short cycle length (manual stimulator control; filled circles). After a pause of several seconds, the fibre was again stimulated for three additional beats, but at a fixed rate. The open circles represent this second train which was initiated while $[K]_o$ was still elevated from the first train of stimuli. The first beat in this case coincidently had an a.p.d. close to the equilibrium value for this cycle length, and no alternans was detected. (Temperature was 22 °C.)

An additional panel (*D*) shows data at 20 °C, but where the K^+ electrode tip is in a position where it measures very small beat-to-beat changes for this temperature (compare to panel *C*). The shortest duration action potential (shown by the open circle) deviates noticeably from a smooth curve connecting the other points. The reason for the apparent bending of the curve and position of this point is treated in the discussion.

We will try to show below how the apparent linearity in the relationship between $[K]_o$ and a.p.d., (disregarding some scatter due in part to resolution of the measurement) represents the underlying similarity in the $[K]_o$ diastolic decay and the restitution curve following each beat. Restitution curves are plots of a.p.d. of a test action potential *versus* diastolic interval between the test action potential and a preceding control action potential. They are described in more detail in Boyett & Jewell (1980), and Colatsky & Hogan (1980). (See also Fig. 4 below.)

Thus if we plot, *versus* one another, two parameters (post-beat $[K]_o$ decay and a.p.d. restitution curve), where both decay exponentially with time, the plot will approach a line as the difference in the time constants of the two parameters approaches zero. (For processes based on two exponentials to approach linearity, we require both time constants and, in addition, the ratios of the coefficients of the exponential terms to approach equality.)

To understand this more clearly, we first performed a simplified version of the experiments that were plotted in Figs. 1–3. Rather than looking at transient responses to sudden increases in rate, we stimulated the fibre at a constant rate (S1 beats) and then, once the a.p.d. had equilibrated at this rate, inserted S2 beats at varying times during diastole.

Results of an experiment comparing $[K]_o$ and a.p.d. during timed extrasystoles are represented in Fig. 4. The preparation was stimulated for a prolonged period at a regular stimulus interval (2·5 sec). The S2 beats were inserted every sixth S1 beat at different intervals following the S1 beats. Plots were made comparing the a.p.d. of the S2 beat to the S1–S2 interval, defined here as the interval between S1

repolarization and the S2 beat upstroke (see Fig. 4; each filled circle represents an action potential).

The time course of uninterrupted diastolic decay of $[K]_o$ (the tail of the beat-to-beat changes following each S1) is indicated by the continuous line on the same graph. This decay of $[K]_o$ was the same for all the S1 diastoles for which no S2 was inserted,

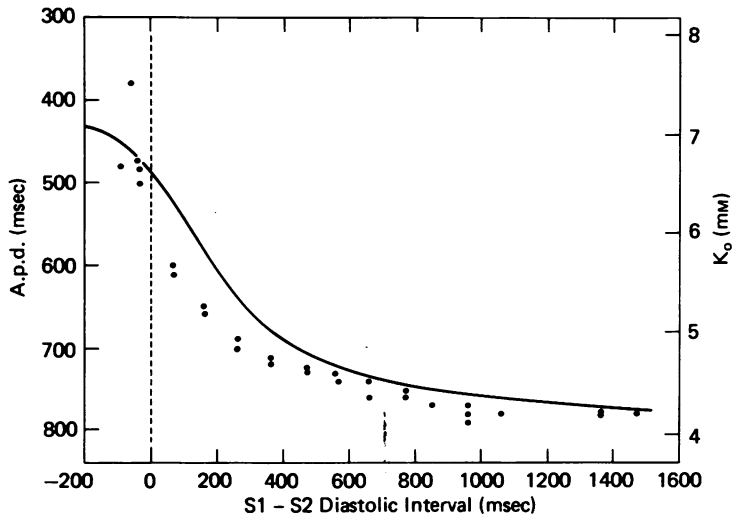

Fig. 4. The filled circles represent the S2 a.p.d.s (left vertical axis in milliseconds) *versus* the S1–S2 diastolic interval on the horizontal axis (see Methods). The S1–S2 diastolic interval is the time between repolarization of the S1 beat and the upstroke of the S2 beat. S2 beats to the left of the dashed vertical line are beats started before the end of the S1 beat, i.e. with zero diastolic interval. The continuous line in the figure represents (right vertical axis) the decay of $[K]_o$ (mM) during diastole. The same $[K]_o$ time course was measured following all S1 beats. Temperature 31 °C.

and therefore reproduceably represented the $[K]_o$ at the start of any S2 beats for all S1–S2 intervals. It can be seen from Fig. 4 that the shapes of the $[K]_o$ decay curve and the S2–a.p.d. curve are quite similar.

Fig. 5 represents the relationship between a.p.d. and $[K]_o$ at the start of the action potential for the experiments on S2 beats (see Fig. 4). The filled circles represent the S2 beats as described above. To determine whether the same relationship between $[K]_o$ and a.p.d. holds for the S1 beats following the S2 beats (S1′), data for several such beats are plotted on the same figure, as open circles. The interval between S1 and S1′ was the same as the interval between any other two control S1 beats with no S2 beats inserted. Note that the open circles fall on the same line as the filled circles. Points which deviate markedly from the curve in Fig. 4 or the straight line in Fig. 5 correspond to action potentials which were premature, i.e. initiated during the action potential plateau of the preceding beat.

For S1′ beats $[K]_o$, which was already elevated at the start of the S2 beat, accumulated further during the S2 beat, and had begun to subside again by the time the next S1 beat came. The plot in Fig. 4 is thus not merely a coincidental correlation due to the similarity of the two time constants in Fig. 4, since the decay of additional

$[K]_o$ following S2 beats now also affects the a.p.d. of these S1′ beats. The implication, which will be developed below, is that these results imply some constraints on the $[K]_o$ level at the end of the beat, in addition to the time course of $[K]_o$ decay following the beat.

Since the diastolic decay of $[K]_o$ for each beat at a constant rate is the same, i.e. the beat-to-beat changes are stable and reproducible, the near linear relationship of

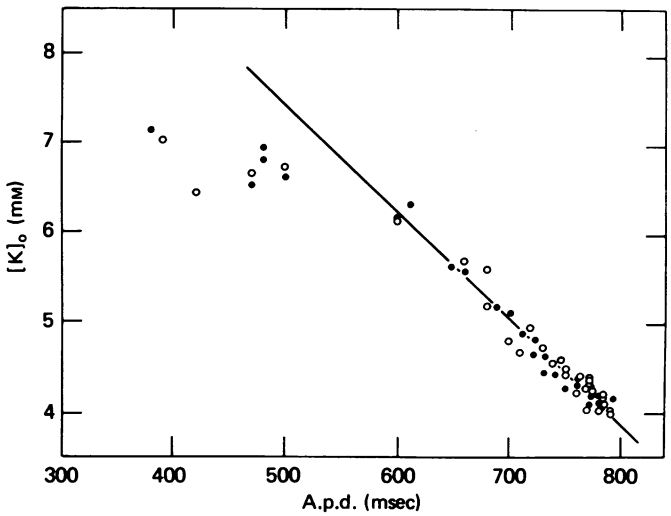

Fig. 5. A.p.d. (horizontal axis in milliseconds) was plotted directly *versus* the $[K]_o$ (vertical axis; mM) at the start of each beat. Filled circles represent the S2 beats. The open circles represent the S1 beats following S2 beats. These S1 beats were initiated while $[K]_o$ was still elevated from the previous S2 beat and were therefore shorter than the normal S1 beats. Beats with a.p.d. shorter than 550 msec were initiated during the action potential of the previous beats and do not fall on the continuous line.

$[K]_o$ and a.p.d. (Fig. 5) is a consequence of a similar decay time constant or constants for the $[K]_o$ decay and the a.p.d. restitution curve. However, during a.p.d. alterations following onset of rapid beating, or in response to a varying stimulus interval, it is not necessarily expected that there is a unique relation between temporal position in the diastolic interval and the $[K]_o$ value, i.e. that the $[K]_o$ tails following all beats are identical. Both the level of $[K]_o$ (at the point of action potential repolarization) and its subsequent time course of decay could be expected to vary. Nor is it necessarily expected that the restitution curves following each beat would be the same for these stimulus conditions.

To clarify this point, we examined $[K]_o$ post-beat decay tails for various short trains of rapid stimulation with a.p.d. alternans. Fig. 6 shows such analysis of $[K]_o$ tails using the same records plotted above in Fig. 3*A*. Fig. 6*A* shows a comparison between the $[K]_o$ decay tail following a single beat (*a*) and that following a train of twelve beats (*b*) at cycle length 330 msec. (See inset to panel *A* for a record of the single beat $[K]_o$ fluctuation – indicated by *a*).

It can readily be seen that the post-train decay tail (*b*) is slower than that following a single beat (*a*). To analyse the mechanism underlying this variation in $[K]_o$ decay,

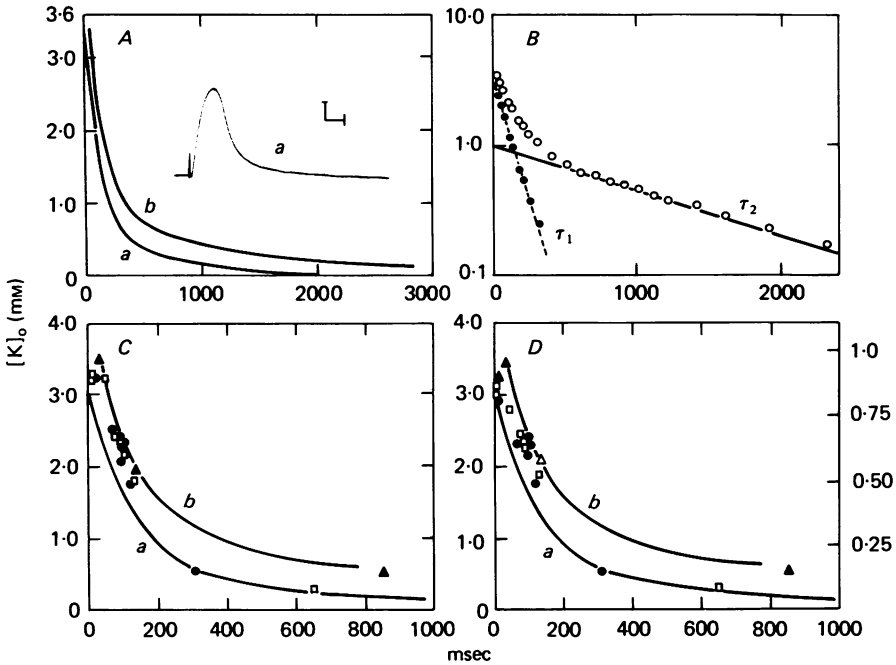

Fig. 6. *A*, insert (*a*) shows K^+ electrode output during a single isolated action potential. Vertical calibration marking is 2 mV. Horizontal is 200 msec. Traces (*a*) and (*b*) are the decay tails of $[K]_o$ accumulation following a single beat (*a*; see insert *a*, this panel) and following a train of twelve beats at cycle length 330 msec (*b*). K^+ electrode recordings are converted to mM-$[K]_o$ and plotted on the vertical axis against time (on the horizontal axis) in milliseconds. (Zero time is taken at 90% repolarization of the final action potential.) *B*, the trace *b* from *A* is fitted using two exponentials where $\tau_1 = 115$ msec and $\tau_2 = 1247$ msec. *C*, shows data points for $[K]_o$ at the start of each beat. Each point is plotted on the horizontal axis *versus* time in milliseconds when the beat occurred. Zero time is taken at 90% repolarization of the previous action potential. Data are from the three stimulus trains in Fig. 3 using the same symbols for each train as in that Figure. The superimposed trace (*a*) is the same as in *A*. Trace *b* is the slowest decay tail for the three trains and is not the same as trace *b* in *A*. *D*, the left vertical and horizontal axis are identical to *C*. However, now points on the right vertical axis represent the change in a.p.d. for all the action potentials for which $[K]_o$ was plotted in *C*. '0' represents no change, and '1' represents maximum change (shortening).

we exponentially split these tails. Two time constants gave the best fit as indicated by computer analysis of the significance level. Panel *B* shows such decomposition of the slower tail (Fig. 6*A*, trace *b*). All tails were fitted by the function:

$$C_1 \exp(-t/\tau_1) + C_2 \exp(-t/\tau_2)$$

where τ_1 varied between 100 and 140 msec and τ_2 between 800 and 1250 msec for these trains of up to twelve beats. The apparent slowing of the decay can be shown from this analysis to result from 'loading' of the slower component, i.e. increasing the ratio of C_2/C_1 from 0·18 for isolated beats to 0·49 for the tail immediately following the longest train. C_1 remained nearly constant for all these beats. For isolated beats during the post-train decay of $[K]_o$, the ratio C_2/C_1 decreased as the test beats were

stimulated further out on this tail, i.e. with smaller initial $[K]_o$. At lower temperatures, both time constants are slower and significant loading of the slower component (C_2) occurs even during single beats. The low temperature action potentials are often lengthened to up to 4 sec, thus allowing more time for the slower components to load.

We now plot values of $[K]_o$ at the start of all beats (both isolated beats and those during trains) *versus* the previous diastolic interval (see Fig. 6*C*; we use the same symbols as Fig. 3*A*). Likewise we also plot (Fig. 6*D*) all a.p.d.s *versus* previous diastolic interval. (The change in a.p.d. is normalized to 1; 0 is no change and 1 is maximum change). Superimposed on these plots are the fastest and slowest decay tails of $[K]_o$. We can see that points on both graphs fall between the two extreme tails. However, from examination of these plots, it can be seen that, even though there is some variation in the $[K]_o$ decay and the restitution curve for different beats during these stimulus protocols, the $[K]_o$–a.p.d. relation is still maintained (see Fig. 3*A* above).

Peak $[K]_o$ during all beats was fairly constant, with maximum variation about 10 % (0·4 mM). This constancy in peak $[K]_o$ during each beat can also be seen in the records of the short rapid train (Fig. 2). However, this phenomenon is not always seen; for example, the peak $[K]_o$ rises slightly during the beats in Fig. 1 (see Discussion).

$[K]_o$ profile during an action potential

To examine in greater detail the relationship betwen $[K]_o$ and a.p.d., we display superimposed (see Fig. 7) a normal action potential (panel *A*, trace 1) and a single shortened action potential (panel *A*, trace 2) along with their respective $[K]_o$ transients (Fig. 7*B*; trace numbers correspond to panel *A*). The second beat is shortened by being initiated following a greatly reduced diastolic interval. It is easy to see by inspection that, whereas final repolarization occurs at approximately the same potential for both action potentials, the plateau for the shortened beat is negative to the primary beat for all but the first 40 msec following the upstroke. At the point of repolarization of the shortest beat, its plateau is about 20 mV negative to the plateau level of the primary beat.

The K^+ electrode output during these two beats is converted to $[K]_o$ values and displayed on the same time scale as the respective action potentials (Fig. 7*B*). It can be seen that the peak $[K]_o$ is the same for each beat, even though $[K]_o$ levels were already elevated at the start of the second beat. In addition, peak $[K]_o$ occurs slightly prior to repolarization for beat 2. (Between peak $[K]_o$ and repolarization, there is a slight decrease in $[K]_o$).

To assist in visually comparing the rate of $[K]_o$ change at the start of each of the two beats, we shift the $[K]_o$ trace no. 2 in a negative direction along the vertical axis so that the initial segment of both $[K]_o$ traces nearly superimpose (trace labelled $2\Delta K$). This visual analysis indicates a reduced rate of $[K]_o$ change during the shortened beat (2); i.e. the slope of the $[K]_o$ trace is less for beat 2 than beat 1. However, one must distinguish between the rate of efflux of K^+ and the slope of the $[K]_o$ profile ($d[K]_o/dt$). The $d[K]_o/dt$ term includes both the net transmembrane efflux of K^+ and the K^+ loss due to diffusion. At different $[K]_o$ levels, different $[K]_o$ gradients imply differing rates of diffusional K^+ loss. Thus, one might obtain a more accurate estimate of the rate of net K^+ efflux by looking at $d[K]_o/dt$ for two situations where

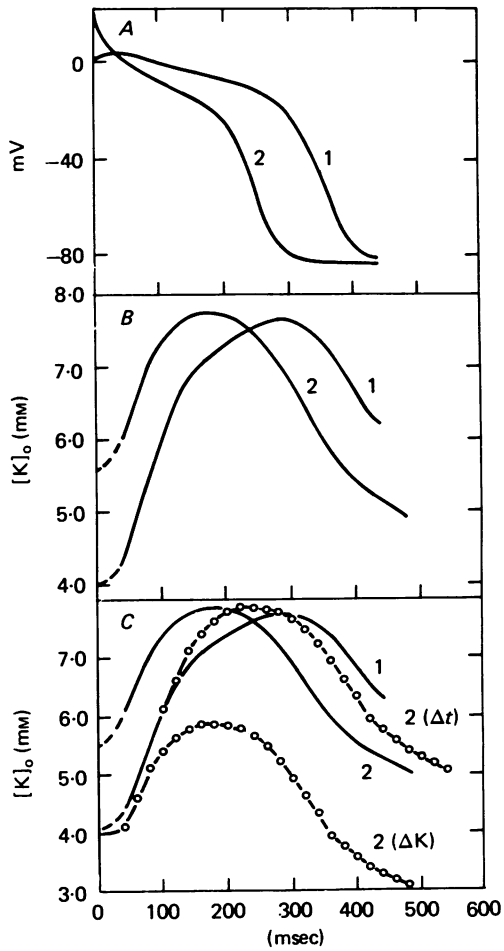

Fig. 7. This figure shows digitized and displayed *versus* the same horizontal axis (time in milliseconds) the membrane potential time course (*A*) and $[K]_o$ values (converted from K^+ electrode output; (*B*) during a normal beat (cycle length 2000 msec; trace labelled 1) and a shortened extrasystolic beat inserted prematurely (diastolic interval less than 100 msec). The dashed lines indicate that the exact voltage trajectory is uncertain due to a stimulus artifact. In *C*, we compared traces 1 and 2 from *B* with the following two display manoeuvres: (1) trace labelled 2(ΔK), open circles, is just trace 2 shifted in a negative direction on the vertical axis so we can visually compare relative $d[K]_o/dt$ for each trace; and, (2) trace 2(Δ*t*), open circles, is just trace 2 shifted 60 msec positive on the horizontal time axis so we can compare relative $d[K]_o/dt$ for identical $[K]_o$ levels in each trace.

we may at least assume comparable $[K]_o$ gradients and hence comparable K^+ loss due to diffusion. Thus we compare $d[K]_o/dt$ for the two traces at points on the trace where $[K]_o$ is equal. To do this we shift trace 2 to the right by 60 msec on the horizontal axis (Fig. 7*C*, trace 2(Δ*t*). Comparing $d[K]_o/dt$ now, we find an increased slope for the $[K]_o$ trace no. 2. From our tail component analysis in Fig. 6, we can derive a procedure for estimating relative rates of efflux for all times during a beat. Such analysis indicates a higher rate for the shorter beat (see Discussion).

Effects of prolonged beating on a.p.d.

It has been previously shown that for prolonged rapid beating, the envelope of $[K]_o$ accumulation plateaus after about one minute and slowly subsides after several minutes of beating (in the temperature range 34–37 °C; Kline *et al.* 1980). A.p.d. shortens during this entire period of rapid drive. Upon return to the slower rate of stimulation, the time required for a.p.d. to return to control values is comparable

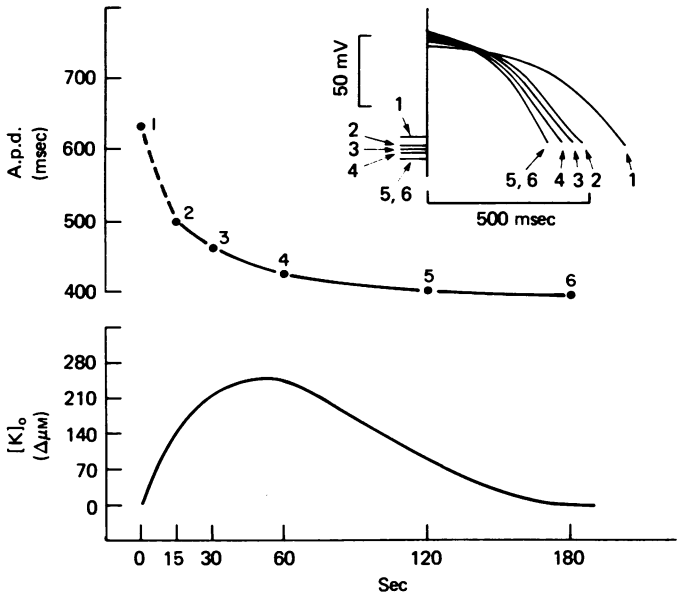

Fig. 8. The bottom graph shows the change in $[K]_o$ (μM) during a 3 min train of rapid stimulation (vertical axis). The horizontal axis shows the time into the stimulation period (duration of drive). The top graph is a continuous plot of a.p.d. (top vertical axis in milliseconds) against the same horizontal axis. Points numbered 1, 2, 3, 4, 5 and 6 correspond to sample action potentials photographically superimposed at various times during the long train and displayed in inset (top right). The dashed line between the points 1 and 2 is the period during which the alternans typically occurs; and so a.p.d. values do not fall on the line, but alternate above and beneath it until they converge.

to the duration of the $[K]_o$ undershoot (Kline *et al.* 1980). Fig. 8 represents changes in a.p.d. and $[K]_o$ continuously monitored during the initial 3 min of rapid stimulation. ($[K]_o$ was monitored at an extracellular location where beat-to-beat changes were not seen.) Numbered points represent the times along the curve at which action potentials were sampled; they are displayed superimposed in the inset (top right). A.p.d. shortening was continuous between points 2 and 6. A hyperpolarization of the membrane potential of about 8 mV is shown schematically in the inset (V_m; see Kline *et al.* 1980). A.p.d. changes between points 1 and 2 (top graph, Fig. 8) often responded with an alternans. This alternans phenomenon is described in detail above. The alternans eventually converged to some average value represented by action potential no. 2.

Effects on m.d.p.

In the next series of experiments, we simultaneously monitored extracellular K^+ activity and m.d.p. in slowly automatic Purkinje fibres subjected to trains of stimulation of varying duration. During a short train (18 sec), $[K]_o$ slowly accumulated and m.d.p. depolarized with a comparable time course (see Fig. 9). Following termination of stimulation, m.d.p. slowly repolarized and $[K]_o$ subsided. No $[K]_o$

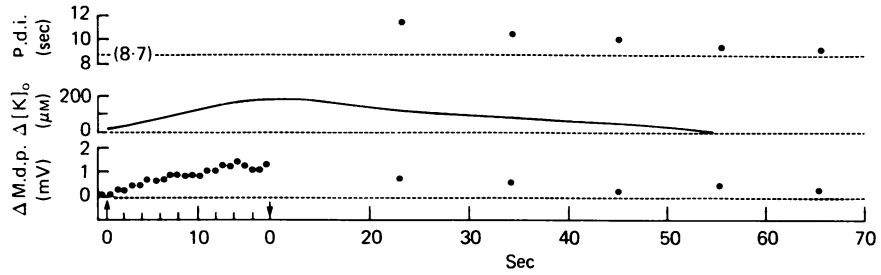

Fig. 9. The three traces (vertical axes) all plotted against the same horizontal axis (time in seconds) indicate: previous diastolic interval (p.d.i. top trace), extracellular K^+ envelope ($[K]_o$, middle trace) and change in m.d.p.. Arrows indicate start ('up' arrow) and termination ('down' arrow) of 18 sec stimulus train (stimulus interval equals 700 msec). Control p.d.i. was 8·7 sec and control m.d.p. was −90 mV. Temperature 35 °C.

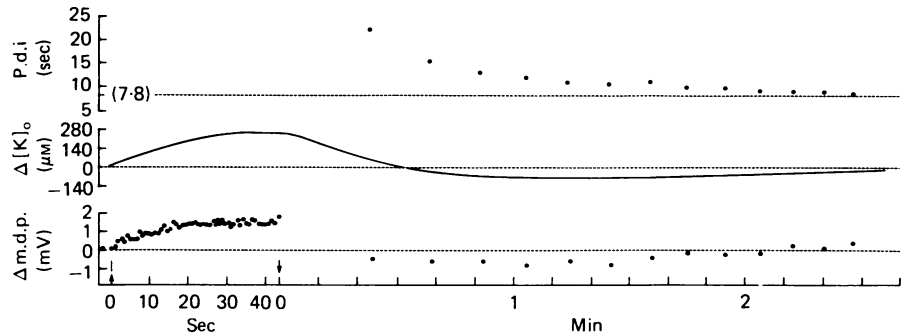

Fig. 10. P.d.i. (top trace), extracellular K^+ envelope ($[K]_o$, middle trace), and change in m.d.p. (bottom trace) are plotted during and after a 45 sec stimulus train (stimulus interval equals 700 msec). Control p.d.i. equals 7·8 sec and control m.d.p. is −90 mV (see caption Fig. 11 and text).

undershoot was observed. When, however, the same fibre was stimulated rapidly for 45 sec, both $[K]_o$ undershoot and m.d.p. hyperpolarization were observed in the post-stimulation period (Fig. 10). These results suggest a relationship between an observable post-stimulation $[K]_o$ undershoot and m.d.p. hyperpolarization, both of which have similar dependence on stimulus duration. In both cases, rapid stimulation suppressed the rate of automatic activity. (Automaticity post-drive is represented as the duration of the previous diastolic interval for each beat plotted on the time axis at the moment the beat occurred).

Fig. 11 represents the result of a typical experiment in which rapid stimulation

was carried out for three minutes. Initially $[K]_o$ accumulated and m.d.p. depolarized, as in the case of a short period of rapid stimulation. M.d.p. reached a maximum level of depolarization while $[K]_o$ continued to increase. M.d.p. then hyperpolarized, slowly crossing the initial pre-stimulus voltage level, while $[K]_o$ was maximal.

With continued stimulation, $[K]_o$ returned to control levels and m.d.p. hyperpolarized further; by 3 min, both attained new equilibrium values. After termination

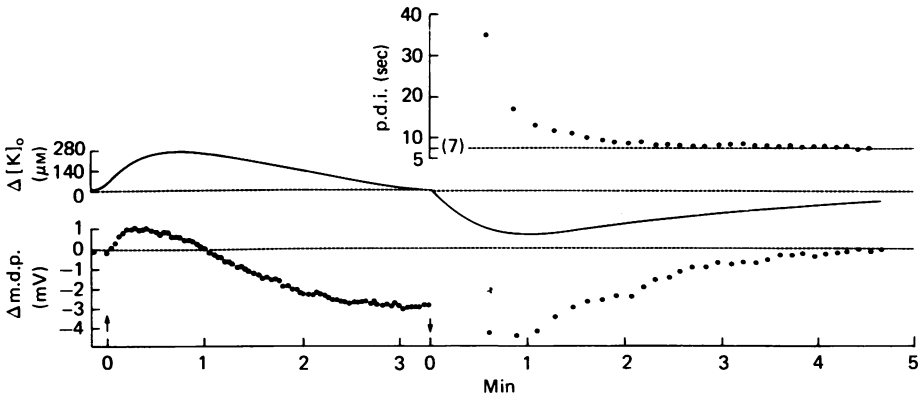

Fig. 11. The bottom trace plots the change in voltage (zero on vertical axis is −90 mV) of the m.d.p. with time (horizontal axis) for a 3 min stimulus train (700 msec stimulus interval). Start of stimulation indicated by 'up' arrow and termination by 'down' arrow. The plot continues for the automatic beats occurring post-drive. The middle trace is the envelope of the $[K]_o$ changes plotted against the same horizontal axis. The upper right tracing is an indication of post-stimulus automatic cycle length plotted against the post-drive segment of the horizontal axis. The p.d.i. is the duration of the preceding diastolic interval for each automatic beat and is plotted on the horizontal axis at the time at which the action potential occurred. The control automatic cycle length (p.d.i. + a.p.d.) is thus slightly larger than 7 sec. Temperature 35 °C.

of stimulation, at this new equilibrium (arrow), further hyperpolarization of m.d.p., followed by a slow return of m.d.p. to control levels, was observed during subsequent spontaneous beating. $[K]_o$ undershoot with a comparable time course, as well as post-overdrive suppression of automaticity, were observed in the post-stimulation period.

Factors affecting post-drive automaticity

We further investigated the suppression of automatic activity after periods of rapid stimulation by direct examination of the trajectories of diastolic depolarization of the membrane potential. With simultaneous measurement of $[K]_o$ undershoot, we have at least inferential indication of the level of Na–K pump activity (Gadsby, 1980; see also Appendix below). We attempted to document the details of change in diastolic depolarization during the post-drive suppression of automaticity, and compare it with changes in $[K]_o$ and estimated state of pump activity, which reproducibly vary during this period.

A fibre that was spontaneously active at a rate of nine beats per minute was stimulated for 60 sec at a rate of eighty-four beats per minute. The first four

spontaneous diastolic membrane depolarizations following stimulation were digitized and compared (Fig. 12*A*). All voltage traces for the diastolic interval were plotted so that the m.d.p.s occurred at the same point on the horizontal time axis. The vertical axis shows voltage changes, where zero corresponds to −90 mV. It can be seen from these tracings that the prolonged diastolic interval is largely due to the

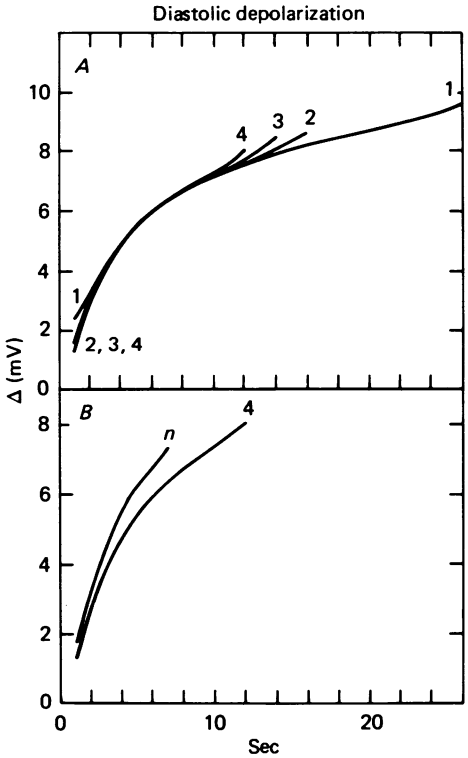

Fig. 12. The change in membrane potential (vertical axis in millivolts; zero corresponds to −90 mV) during diastole is displayed *versus* time (horizontal axis in seconds) for various sample action potentials following a 60 sec train of stimulation (see text). *A* displays the voltage trajectory for the first four post-drive beats. The m.d.p. of beat 1 is more positive than that for beats 2, 3, 4, due to the elevated $[K]_o$ during beat 1. Notice the initial prolongation of the later phases of diastolic depolarization. *B* displays the voltage trajectory for the fourth beat and seventeenth beat. The seventeenth beat is labelled '*n*' and it superimposes with all later beats and also the pre-drive control. Notice the increased rate of diastolic depolarization for beat *n*.

elevation of the take off potential and the elongation of the late phase of diastolic depolarization. The early phases of all the spontaneous beats are nearly superimposable. Analogous to Figs. 10 and 11, all m.d.p.s are hyperpolarized and the m.d.p. of beat 1 is less hyperpolarized than that for beats 2–4.

Panel *B* of Fig. 12 compares by superposition the voltage trace for the fourth post-drive diastolic depolarization with that of a control action potential taken after the overdrive effects had completely subsided. (It also was completely superimposable with the pre-drive control action potential). Three features of post-drive diastolic depolarizations are obvious: (1) the change of take-off potential; (2) the progressive

depolarization of the m.d.p. during the later phases of the post-drive period and (3) the increased slope of the early diastolic depolarization for the beats occurring later in the post-drive period. Slow changes in all three parameters during most of the post-drive period are responsible for the slowly varying automatic rate. During this entire period, the pump rate is decaying with a time constant of approximately 140 sec (see Appendix).

DISCUSSION

The changes in action potential duration with rate of stimulation have been studied here as they relate to two basic mechanisms. First, transient beat-to-beat fluctuations in $[K]_o$ may account for changes in the a.p.d. of extrasystoles and of beats following sudden onset of rapid stimulation. Secondly, a progressive activation of outward currents associated with prolonged drive appears related to activation of Na–K pump. Consideration of these two mechanisms in addition to gated currents and intracellular ionic mediation may help resolve the complex problem of action potential repolarization (Trautwein, 1973; Carmeliet, 1977; Boyett & Jewell, 1980).

Our observations of the effects of beat-to-beat fluctuations in $[K]_o$ on a.p.d. are consistent with observations in frog ventricle by Kline & Morad (1978), and previous predictions by others (Carmeliet, 1955; Weidmann, 1956; Hoffman & Cranefield, 1960; Cleeman & Morad, 1979). The fluctuations in $[K]_o$ which we have documented, during the electrical alternans following the onset of rapid stimulation, have similar kinetics to the changes in time-dependent outward current conductances described by Hauswirth, Noble & Tsien (1972) to explain the alternans in sheep Purkinje fibres. Specifically, exponential filling of restricted diffusion compartments can in many respects mimic exponentially activating Hodgkin–Huxley currents (Attwell *et al.* 1979).

Beat-to-beat variations in $[K]_o$ would be expected to affect a number of physiological parameters in the Purkinje fibre membrane. Such changes would alter the K^+ conductance and shift the K^+ equilibrium potential, thus giving time dependence to the rectifiers of various K^+ channels (Attwell *et al.* 1979). At any given rate of beating, there is continual pump activity restoring the gradient as K^+ and Na^+ ions flow through the passive channels. If this pumping is electrogenic (Gadsby & Cranefield, 1979*a*; Eisner & Lederer, 1979; Kline *et al.* 1980; Cohen *et al.* 1981) and sensitive to $[K]_o$ (Gadsby, 1980), then large beat-to-beat changes in $[K]_o$ would be expected to modulate the steady pump rate contributing fluctuations in outward current during each cycle. Furthermore, shifts in K^+ conductances would modulate the voltages generated by even a constant electrogenic pump rate, by changing the total membrane conductance.

Description of $[K]_o$ *changes*

The $[K]_o$ changes measured during beating can be grouped into two types (see Kline & Morad, 1978). For some K^+ electrode tip positions, only slow changes of $[K]_o$ can be seen (see Fig. 8–11). These are generally of the order 200–700 μM (values of C_3) and have time constants (τ_3) for accumulation and decay on the order of 10–30 sec (see Appendix). For other positions, presumably nearer the membrane, beat-to-beat

$[K]_o$ fluctuations are seen. These decay with two time constants. At 37 °C, the fast time constant (τ_1) is in the range of 90–140 msec for the decay following the beat. The slower time constant (τ_2) range is from 800 to 1250 msec. These numbers for τ_1 and τ_2 are quite comparable to the values for the time constants of the restitution curves described by Colatsky & Hogan (1980) in this same preparation.

The coefficient for the fast change (C_1) was routinely measured to be as large as 3 mM at 37 °C. The coefficient of the slow change (C_2) was about 0·2–0·6 mM for a single beat but could increase to about 1·5 mM during a short train of rapid beating when loading of the compartment was complete. Since at 37 °C the a.p.d. (about 300 msec) is two to three times longer than τ_1 but only about $\frac{1}{3}$ of τ_2; it is expected that during a single beat, the fast component would be fully loaded, but the slow component would need a short train or a very long beat to be fully loaded. During a single beat in a cooled fibre, in addition to loading a greater portion of the slower time constant component, the values of τ_1 and τ_2 are also larger (unpublished observation). This explains the more prolonged effect of a single beat on the a.p.d. of a subsequent beat (i.e. larger restitution curve time constant) at low temperature.

For electrode tip positions where the total beat-to-beat changes are smaller, there is also generally noted a loss of the faster component (τ_1), i.e. C_1 is smaller, or alternatively, the ratio of C_2/C_1 gets larger. In this position, due to the predominance of the τ_2 component, one sees a slight increase in peak $[K]_o$ for the first few beats of a train as the C_2 compartment loads (see Fig. 1). However, for positions of the tip where we measure larger accumulations, we note larger values of C_1. The peaks appear constant during such a short train since the C_1 component, which fully loads during each beat, is dominant (Fig. 2). It is understood that at any particular electrode position, we are only measuring $[K]_o$ fluctuations in one particular extracellular location, and that the a.p.d. for an entire strand of myocytes is determined by some weighted average of $[K]_o$ facing the membrane for the entire electrophysiological cable. Thus in Fig. 3*D*, the rather small beat-to-beat changes measured at this electrode position contained a non-representatively small proportion of the C_1 component. We might then expect the plot of initial $[K]_o$ *versus* a.p.d. (especially for the high $[K]_o$ end of the curve, i.e. the point represented by the open circle) to deviate noticeably from linearity, since we are comparing a restitution curve with a large C_1 component to a $[K]_o$ decay curve where this component is mostly absent (i.e. one curve is dominated by its τ_1 time constant and one by its τ_2 time constant).

Even for electrode tip positions where no beat-to-beat changes are seen, the rate dependence of the slow C_3 component is still consistent with its origin as the summation of the faster $[K]_o$ components which affect a.p.d. For example, as the cycle length for short stimulus trains is slowly decreased, the range from the minimum cycle length at which C_3 accumulation is first seen to the fastest sustainable rates (shortest cycle length) corresponds to the same range of cycle length for which most of the a.p.d. shortening occurs (i.e. rates faster than 60/min, or cycle length equal to 1000 msec; for temperature of 37 °C). At this rate, we have approximately a 700 msec diastolic interval during which more than 92 % (see Fig. 6) of a single beat-to-beat $[K]_o$ change will have decayed.

Anatomical correlates

Although we do not have precise knowledge as to the location of the electrode tip in the extracellular space, this method of analysis gives an approach to studying extracellular $[K]_o$ changes based on kinetics rather than absolute magnitudes of accumulation. In particular, individual components of the $[K]_o$ change are identified which are useful for studying specific electrophysiological parameters. Thus the two fast components associated with the beat-to-beat decay (C_1 and C_2) are relevant for study of the action potential duration. The slow component (C_3) and the undershoot are relevant for study of the m.d.p. and the state of pump activation.

Yet it still may be useful to suggest what features of the extracellular space may be determining these time constants and coefficients. Recently Eisenberg & Cohen (1981) have described the anatomy of the small canine Purkinje fibre as well as performing comparative studies on the large fibres. They have described the average cell diameter as approximately 30 μM; and have indicated that in the large Purkinje fibres, bundles of myocytes are grouped into trabecula, like ventricular muscle. These bundles are loosely packed with myocytes comprising only about 30% of the extracellular volume on average. Furthermore, about $\frac{1}{3}$ of the total cell membrane area faces clefts between 1 and 15 μM wide. Thus we might assign τ_3 to the total radius of the Purkinje fibre (see Appendix); τ_2 to the trabeculae, which would be required to contain about twenty myocytes and be 150–200 μM in diameter; and τ_1 to clefts between small groups of two to three myocytes each. The dimensions of these putative cleft populations are appropriate for the three time constants. Most likely active pumping also modulates the measured time constants.

Action of elevated $[K]_o$ *on a.p.d.*

Having described the kinetics of the $[K]_o$ tails, we must ask how the initial $[K]_o$ elevation causes a.p.d. shortening. This analysis is somewhat complicated by the different voltage trajectory of the two plateaus and the difficulty in determining net K^+ efflux from $d[K]_o/dt$ alone. Fits of the rising phase of the $[K]_o$ beat-to-beat transient (between 20% and 80% of peak $[K]_o$) to a single exponential indicate a slightly faster time constant for the rising phase than the falling phase. One interpretation of this is that the rate of K^+ net efflux is decreasing during the plateau. This is supported by the fact that the $[K]_o$ transient often actually peaks and then starts to decline slightly before rapid repolarization.

Recent experiments in which extracellular K^+ electrodes were used in voltage clamped small canine Purkinje fibres (Cohen *et al.* 1982; Kline, Cohen, Falk & Kupersmith, 1982) indicate a monotonic increase in $[K]_o$ (often in the millimolar range) during 5 sec clamps to the plateau. The magnitude of the accumulation during clamp steps from diastolic holding potentials is larger for more positive plateau potentials where larger outward currents are activated. Thus the slow decrease in potential (negative potential shift) during the plateau acts to reduce net K^+ efflux even while elevated $[K]_o$ acts to increase K^+ efflux for a given potential. At potentials positive to the crossover of the rectifiers of the potassium plateau currents, for a higher initial $[K]_o$, a more negative plateau voltage could generate sufficient outward K^+ current to balance a given level of inward current.

Detailed fitting of the rising phase of these beat-to-beat $[K]_o$ accumulations will not be pursued to the same extent as the fitting of the tails. The plateau efflux is large and changing during the beat, whereas the potential is effectively constant during the tails in non-automatic fibres, and, in addition, the passive diastolic currents are much smaller. (There may also be some additional contribution from very early K^+ currents; see Vereecke, Isenberg & Carmeliet, 1980). The diffusion parameters cannot be accurately determined in the presence of large potassium currents of unknown time dependence, and extrapolation back to the currents from the $[K]_o$ change will be left to another manuscript.

However, we can make several estimates which confirm the initial indications of a greater net K^+ efflux rate during the plateau of the shorter beat (see Fig. 7). First, just prior to the upstroke of the shortened beat, $[K]_o$ is decaying from the first beat with a time constant of approximately 140 msec and is elevated by about 2 mM. We compare the initial $[K]_o$ slope for the two beats during the period from 40 to 80 msec following the upstroke for each beat, and note that the longer beat has a slope about 17% greater. However, correcting for the K^+ loss due to diffusion during this period for the shortened beat (the gradient is much higher for the shortened beat with elevated initial $[K]_o$), we find that we have underestimated the net K^+ efflux of the second beat by about 30%. Thus the efflux rate is larger during the second beat. Secondly, by shifting the $[K]_o$ trace on the time axis to compare the slope of $d[K]_o/dt$ at equal values of $[K]_o$ (see trace $2(\Delta t)$ Fig. 7*C*), we can determine by inspection that the efflux is larger for the second beat for at least the last 200 msec of each action potential. However, the peak $[K]_o$ values during beats in an alternans are often nearly equal. If we assume, therefore, comparable gradients during each beat, this implies that net K^+ efflux is equal at the peak $[K]_o$ for each beat. (K^+ loss due to diffusion is equal due to the equal gradients, and $d[K]_o/dt = 0$ at the peak for both.)

Thus it appears as though, during these short alternans: (1) the higher level of $[K]_o$ during the shortened beat shifts the total membrane *I–V* relation in a positive direction by shifting the K^+ current rectifiers. This new *I–V* relation has a more negative plateau intercept (i.e. the zero current intercept just positive to the inward current window; Jack, Noble & Tsien, 1975. This lowers the plateau of the shortened beat. (2) The greater rate of efflux of K^+ also may contribute to the greater net outward currents evidenced by the larger negative dV/dt of the plateau of the shortened beat. (3) The threshold conditions for ultimate repolarization appear to be related to both a sufficiently negative membrane voltage accompanied by a sufficiently high peak $[K]_o$ value to eliminate the net inward current window negative to this voltage. Since the membrane *I–V* relation is a function of all the currents, the $[K]_o$–a.p.d. curve would be shifted following interventions which significantly affected the magnitude or kinetics of other plateau currents; or, deviations from the curve may occur (for example, at very short diastolic intervals; see Fig. 5) due to the influence of other time dependent processes.

Effects on automaticity

It appears that for short periods of stimulation at rapid rates, $[K]_o$ accumulation accompanies depolarization of the m.d.p. Both $[K]_o$ accumulation and m.d.p. depolarization then subside together following cessation of stimulation. For more

prolonged trains of rapid stimulation, a hyperpolarization of m.d.p. develops during the later stages of rapid stimulation, while $[K]_o$ is still elevated. Following prolonged periods of stimulation, an undershoot in $[K]_o$ is observed. The duration of stimulation at which m.d.p. is seen to start hyperpolarizing is comparable to that minimally necessary to induce a measureable post-drive $[K]_o$ undershoot. Since Kunze (1977) has shown a strong relationship between the $[K]_o$ undershoot and the level of pump activation, we attribute the m.d.p. hyperpolarization to activation of an Na–K pump.

Maximum hyperpolarization during rapid stimulation is observed when the envelope $[K]_o$ has subsided to control values. We assume that at this point pump activation is also maximal and we note that $[K]_o$ is also constant. Upon cessation of beating, a further hyperpolarization is observed along with the $[K]_o$ undershoot. It appears that m.d.p. is reflecting both the $[K]_o$ changes directly and the changing level of currents associated with the decline of the pump post-drive. These findings are consistent with many of the predictions made by Vassalle (1970, 1977) and Browning *et al.* (1979).

That the level of $[K]_o$ *per se* is not the sole determinant of m.d.p. after rapid stimulation is seen in Fig. 11. M.d.p. prior to and at the conclusion of a three minute train of stimulation have quite different potentials, with the post-drive m.d.p. being markedly hyperpolarized. However, $[K]_o$ levels are the same for these two instances. After termination of stimulation, the first few automatic beats have the same $[K]_o$ value as corresponding beats during the rising phase of $[K]_o$ at the end of the undershoot. Yet these beats, with similar $[K]_o$ values, have markedly different m.d.p.s and diastolic membrane potential trajectories.

Although the hyperpolarization of m.d.p. may be accounted for by changes in the level of activation of the Na–K pump and the effects of $[K]_o$ on the K^+ equilibrium potential, it is also possible that intracellular Na^+ elevation *per se* plays a role in determining m.d.p., for example by: (1) reduction of the inward background currents; or (2) secondary elevation in intracellular Ca^{2+} which then affects the K^+ conductance.

Alternatively, the changes in level of pump activation may alter the $[K]_o$ diastolic trajectory by changing the rate at which beat-to-beat $[K]_o$ fluctuations subside. DiFrancesco (1981) has now reported that the pacemaker is an inward current turning on in the presence of additional currents which are generated by $[K]_o$ depletion modifying the conductance of the background K^+ channel. Thus, differential pump effects on the rate of diastolic $[K]_o$ decay may affect diastolic currents by modulating this $[K]_o$ depletion. In this study the diastolic voltage trajectory is shown to be constantly varying during the post-drive period in ways which cannot be explained solely by variations in the m.d.p. level, but would also seem to include direct or indirect effects of the Na–K pump. For example, at these diastolic potentials below the crossover of the I_{K_1} rectifier, $[K]_o$ depletion causes larger outward potassium currents which would slow diastolic depolarization, as would the direct effects of electrogenic outward currents.

APPENDIX

Efforts at modelling extracellular K^+ accumulation in nerve and muscle preparations have met with some success (DiFrancesco & Noble, 1979; Pape & Katzman,

1972; Cleeman & Morad, 1979; Lux & Neher, 1973; Freygang, Goldstein, Hellam & Peachey, 1964; Langer & Brady, 1966).

We have attempted to account for the observed time course of extracellular K^+ accumulation with a mathematical model which treats the larger extracellular spaces (C_3 component) of the Purkinje fibre bundle as a homogeneous cylindrical space of given finite radius and infinite length. At any given radial depth within the fibre bundle, net transmembrane K^+ efflux, which rapidly alters the smaller cleft concentrations (most likely those components identified by C_1 and C_2), eventually diffuses into the larger extracellular spaces. The instantaneous rate of change in extracellular K^+ concentration ($d[K]_o(t)/dt$) caused by this diffusion into the larger spaces is represented in the diffusion equation by a time dependent exponentially decaying function. Thus we are modelling here the slow $[K]_o$ changes shown in Figs. 8–11 where no beat-to-beat $[K]_o$ fluctuations were seen. (A more complex simulation model treating both clefts and the larger extracellular spaces is described in Cohen & Kline, 1981; the model below allows for analytical solutions which generate estimates of pump activity.)

The net K^+ efflux is derived from both passive K^+ currents and active K^+ uptake (the Na–K pump). From the recent reports by Deitmer & Ellis (1978), Gadsby (1980) and Cohen *et al.* (1981), a reasonable estimate of the state of pump activation during a prolonged train of beating would be to use an exponential function of the form:

$$M(t) = -p(1-\exp(-\lambda t)). \tag{1}$$

Since we know that after several minutes of beating, the overall net efflux of K^+ is zero and $[K]_o$ has returned to bath levels (see Figs. 8 and 11), the fully activated pump flux must equal the passive K^+ efflux for $t > 180$ sec. If we assume that the passive fluxes are constant during a train of rapid beating, and that the difference in the passive fluxes induced by the rapid beating is described by 'j', then the total flux becomes:

$$M(t) = -p(1-\exp(-\lambda t))+j. \tag{2}$$

However, for $M(t > 180) = 0$, we must have $p = j$, and thus eqn. 2 becomes:

$$M(t) = j\exp(-\lambda t). \tag{3}$$

Thus the instantaneous rate of change in K^+ concentration ($d[K]_o(t)/dt$), due to the net K^+ efflux, is represented in the diffusion equation by $j\exp(-\lambda t)$ where j is given in units of mM/sec (i.e. corrected for ratio of membrane area/cleft volume). As noted above, the slow $[K]_o$ changes are quite small (several hundred micromolar) and thus we assume that the efflux $M(t)$ is independent of them. Thus, this efflux term is only dependent on 't' and not the radial position, r. This is an important assumption, and allows us to eventually solve for the $[K]_o$ (r, t) as the product of two separate functions, one in r and one in t (Crank, 1956). Thus the actual radial depth of the electrode tip is not important for the time course of the $[K]_o$ change. Implicit in this assumption is the further assumption that the beat to beat changes merely superimpose on the very much smaller slow changes and thus, their contours are also radially independent.

With these considerations in mind, we are left to solve the following diffusion equation in cylindrical co-ordinates:

$$d[K]_o(r,t)/dt = -D(d^2/dr^2 + (1/r)\,d/dr)[K]_o(r,t) + j\exp(-\lambda t). \quad (4)$$

Solutions for this equation are given by Carslaw & Jaeger (1959) where $\beta \cong D\alpha_1^2$ and $J_o(a\alpha_n) = 0$:

$$[K]_o(r,t) = (j/\lambda)\,e^{-\lambda t}\left[\frac{J_o[r(\lambda/D)^{\frac{1}{2}}]}{J_o[a(\lambda/D)^{\frac{1}{2}}]} - 1\right] - \left(\frac{2j}{a}\right)\sum_{n=1}^{\infty}\frac{e^{-D\alpha_n^2 t}\,J_o(r\alpha_n)}{\alpha_n(D\alpha_n^2-\lambda)J_1(a\alpha_n)} + [K]_o(a) \quad (5)$$

we examined values of the Bessel function radial terms to see whether we could neglect all but the left hand term in eqn. (5) and the first term in the expansion (right hand term, $n = 1$). The errors in neglecting higher order terms would be the most significant at time zero, where $[K]_o(r,0) = 0$. At $r = 0$ and $t = 0$, this error is about 3% using the estimated values of the time constants. At $r = 0{\cdot}95a$ (a is the radius of the preparation), the error at $t = 0$ is about 13%. However, this is so near the edge that the changes in $[K]_o$ are about 10% of those measured at the centre and this error could probably not be detected. Thus we find by examining the radial terms at different r values, an acceptably small error in estimating the diffusion profile by the product of one radial term (which is the first Bessel expansion coefficient; $n = 1$), and a second term containing all the time dependence. This second term is the difference in two exponentials. Analysis of the derivation of the equation shows that the time constants of these two exponentials correspond to the pump activation time constant ($1/\lambda$) and the standard diffusion time constant of the cylinder ($1/\beta$).

Fig. 13*C* shows a fit (to the difference in two exponentials) of the $[K]_o$ profile measured with an extracellular K^+ sensitive electrode during a three minute train. The open circles represent digitized data points which were converted into $[K]_o$. The continuous line is computer drawn and is the difference of two exponentials. The time constant of the diffusion term is fitted to be 29·4 sec. We also estimated this time constant by fitting the decay of $[K]_o$ following a short period of stimulation at the same rate and for the same puncture position. The stimulation period was short enough so that following it no undershoot of $[K]_o$ could be detected. The value estimated this way was 27 sec. This corresponds to a fibre diameter of approximately 1 mm (assuming no tortuosity; about 700 μM assuming maximum tortuosity). Thus interpreting this term as representing the radial diffusion time constant appears quantitatively reasonable.

The fit of the second time constant, the pump activation time constant, was 62·5 sec (Fig. 13*C*). As an independent estimate of this term, we looked at the dependence of the prolongation of the first post-drive automatic diastolic interval on the duration of the preceding stimulus train. Thus we assumed that the prolongation of the first post-drive beats was proportional to the amount of intracellular Na^+ loading. A plot of these two parameters is shown in Fig. 13*A* for thirteen stimulus trains applied in random order. (The same fibre and stimulation rate is used as in Fig. 13*C*). The smooth curve through the points represents the computer fit to a single exponential:

$$\text{d.i.} = 37(1-\exp(-\lambda t)) \quad (6)$$

where d.i. is diastolic interval. The fit value for λ is 0·0168 (time constant is 59 sec) and t is the preceding drive duration.

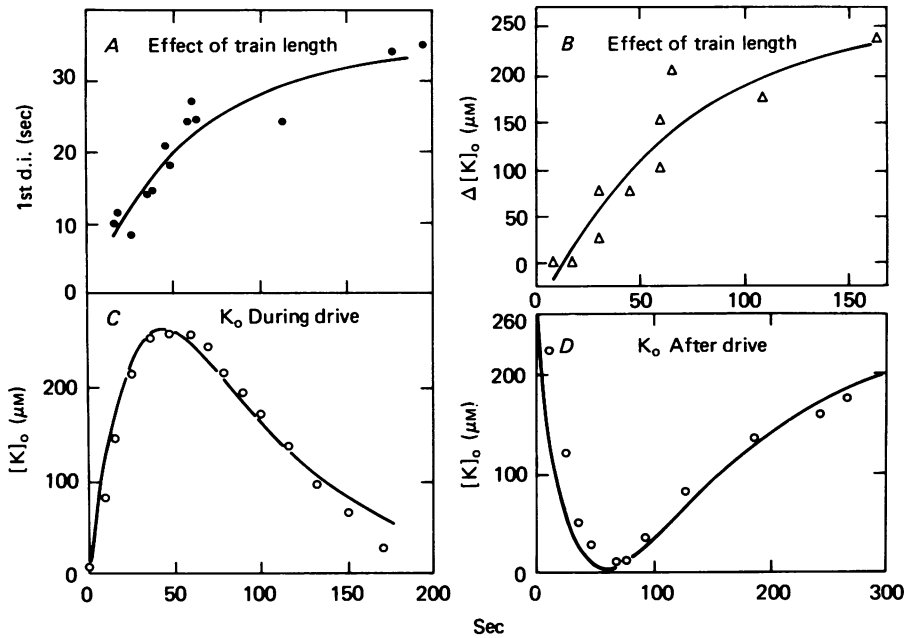

Fig. 13. In *A* we plot the duration of the first diastolic interval (d.i.; the time to the first post-drive automatic beat; vertical axis) *versus* the length of the preceding stimulus train (horizontal axis in seconds) for thirteen trains of varying duration but identical rates (1 beat per 700 msec; filled circles). The continuous line is a computer drawn exponential fit of these points to the function: $f(t) = b - a\exp(-\lambda t)$; where $a = 34{\cdot}23$, $b = 34{\cdot}98$ and $\lambda = -0{\cdot}0169$ (i.e. time constant = 59 sec). The duration of drive is 't'. *B*, values of maximum amount of $[K]_0$ depletion (in mM-$[K]_0$ below base line) for ten trains (cycle length equals 700 msec) of varying length applied in random order (open triangles). The smooth curve is a computer fit of the points to the function $A(1-\exp(-\lambda t))$ with values of $A = 266$ μM and $\lambda = 0{\cdot}01429$ (i.e. time constant of 70 sec). *C*, the open circles represent digitized values of the elevation of the $[K]_0$ envelope during 3 min of continuous beating, plotted against the same horizontal axis (sec). The solid line is a computer drawn fit of these points to the function: $[K]_0(t) = c(\exp(-\lambda t) - \exp(-\beta t))$; where $c = (3{\cdot}55) \times (275\ \mu M)$, $\beta = 0{\cdot}034$, and $\lambda = 0{\cdot}016$ (i.e. time constant is 62·5 sec). *D* is a fit of the post-drive depletion using the difference of two exponentials and constraining $1/\beta$, the diffusion time constant, to values obtained in *C*. The new value of λ is 0·007 (i.e. time constant = 142 sec).

In addition, we fit the magnitude of the $[K]_0$ depletion following these trains plotted against the duration of the train (Fig. 13*B*). Although there is some scatter in these points, the value of λ is 0·01429 (time constant of 70 sec) which is close to the other two estimates whose values were 59 and 62·5 sec. These estimates of the pump activation times are quite similar to values from Gadsby (1980), Kline *et al.* (1980), and Cohen *et al.* (1981).

Thus it appears that the amount of pump activation at the termination of the train has a direct effect on at least the prolongation of the first beat and that the amount of activation is exponentially dependent on the prior drive duration. However, the kinetics of the pump decay in the post-drive period does not have the same time constant as the loading of the pump estimated above. Fig. 13*D* shows a fit of the

$[K]_o$ undershoot. The same value of β is obtained, as expected, but the λ value is much smaller (0·007; time constant is 142 sec). This variation may be due to different average values of $[K]_o$ in the clefts during the post-drive period where there are significantly fewer large $[K]_o$ excursions due to beat-to-beat efflux.

We would like to thank Stuart Dickerman for technical assistance with the experimentation and data analysis, and Michael Siegal, Ira Cohen, and Mitch Baker for helpful discussions at all stages of this work. R.P.K. was supported by a Young Investigator Award (no. 25798) from N.I.H.L.B.I. and a grant (no. 80 909) from the American Heart Association. J.K. was supported by grant no. 25135 from the N.I.H.L.B.I., a grant in aid from the New York Heart Association, and the Hearst Foundation.

REFERENCES

ATTWELL, D., EISNER, D. & COHEN, I. (1979). Voltage and tracer flux data: the effects of a restricted extracellular space. *Q. Rev. Biophys.* **12**, 213–261.

BAUMGARTEN, C. & ISENBERG, G. (1977). Depletion and accumulation of potassium in the extracellular clefts of Purkinje fibers during voltage clamp hyperpolarization and depolarization. *Pflügers Arch.* **368**, 19–31.

BOYETT, M. R. & JEWELL, B. R. (1980). Analysis of the effects of rate and rhythm upon electrical activity in the heart. *Prog. Biophys. molec. Biol.* **36**, 1–52.

BROWNING, D. J., TIEDMAN, J. S., STAGG, A. L., BENDITT, D. G., SCHEINMAN, N. N. & STRAUSS, H. C. (1979). Aspects of rate-related hyperpolarization in feline Purkinje fibers. *Circulation Res.* **44** (5), 612–624.

CARMELIET, E. (1955). Influence du rhythme sur la durée du potential d'action ventriculaire cardiaque. *Archs int. Physiol. et Biochem.* **63**, 222–232.

CARMELIET, E. (1977). Repolarization and frequency in cardiac cells. *J. Physiol., Paris* **73**, 903–923.

CARSLAW, H. S. & JAEGER, J. C. (1959). *Conduction of Heat in Solids*, section 7.9, p. 204. Oxford: University Press.

CLEEMAN, L. & MORAD, M. (1979). Extracellular accumulation in voltage-clamped frog ventricular muscle. *J. Physiol.* **286**, 83–111.

COHEN, I., DAUT, J. & NOBLE, D. (1976). The effects of potassium and temperature on the pacemaker current iK_2 in Purkinje fibres. *J. Physiol.* **260**, 55–74.

COHEN, I., EISNER, D. & NOBLE, D. (1978). The action of adrenaline on pacemaker activity in cardiac Purkinje fibres. *J. Physiol.* **280**, 155–168.

COHEN, I., FALK, R. & KLINE, R. P. (1981). Membrane currents following activity in canine cardiac Purkinje fibers. *Biophys. J.* **33**, 281–288.

COHEN, I., FALK, R. & KLINE, R. P. (1982). Pacemaker activity in cardiac Purkinje fibers: a voltage clamp analysis. In *Normal and Abnormal Conduction in the Heart* ed. HOFFMAN, B. F., CARVAHLO, P. D. & LIEBERMAN, M. (in the Press).

COHEN, I. & KLINE, R. (1981). K^+ accumulation in the extracellular spaces of cardiac muscle: evidence from voltage clamp and extracellular K^+ selective micro-electrodes. *Circulation Res.* (in the Press).

COLATSKY, T. J. & HOGAN, P. M. (1980). Effects of external calcium, calcium channel-blocking agents, and stimulation frequency on cycle length-dependent changes in canine cardiac action potential duration. *Circulation Res.* **46** (4), 543–552.

CRANK, J. (1956). *Mathematics of Diffusion*. Oxford: University Press.

DEITMER, J. W. & ELLIS, D. (1978). The intracellular sodium activity of cardiac Purkinje fibres during inhibition and re-activation of the Na–K pump. *J. Physiol.* **284**, 241–259.

DIFRANCESCO, D. (1981). A new interpretation of the pace-maker current in calf Purkinje fibres. *J. Physiol.* **314**, 359–376.

DIFRANCESCO, D. & NOBLE, D. (1979). On the time course of extracellular ion concentration changes in frog atrium. *J. Physiol.* **296**, 80*P*.

EISENBERG, B. & COHEN, I. (1981). Morphometric analysis of dog Purkinje strands. *Biophys. J.* **33**, 35a.

EISNER, D. & LEDERER, W. (1979). The role of the sodium pump in the effects of potassium depleted solutions on mammalian cardiac muscle. *J. Physiol.* **294**, 279–301.

FREYGANG, W. H. JR., GOLDSTEIN, D. A., HELLAM, D. C. & PEACHEY, L. D. (1964). The relation between the late after potential and the size of the transverse tubular system of frog muscle. *J. gen. Physiol.* **48**, 235–263.

GADSBY, D. C. (1980). Activation of electrogenic Na^+/K^+ exchange by extracellular K^+ in canine cardiac Purkinje fibers. *Proc. natn. Acad. Sci. U.S.A.* **77**, 4035–4039.

GADSBY, D. C. & CRANEFIELD, P. F. (1979*a*). Direct measurement of changes in sodium pump current in canine cardiac Purkinje fibers. *Proc. natn. Acad. Sci. U.S.A.* **76**, 1783–1787.

GADSBY, D. C. & CRANEFIELD, P. F. (1979*b*). Electrogenic sodium extrusion in cardiac Purkinje fibers. *J. gen. Physiol.* **73**, 819–837.

HAUSWIRTH, O., NOBLE, D. & TSIEN, R. W. (1972). The dependence of plateau currents in cardiac Purkinje fibres on the interval between action potentials. *J. Physiol.* **222**, 27–49.

HOFFMAN, B. F. & CRANEFIELD, P. F. (1960). *Electrophysiology of the Heart.* New York: McGraw-Hill.

JACK, J. J. B., NOBLE, D. & TSIEN, R. W. (1975). *Electric current flow in excitable cells.* Oxford: Clarendon Press.

KLINE, R. P. (1975). K^+ efflux and accumulation in frog ventricular myocardium. *Ph.D. thesis*, University of Pennsylvania.

KLINE, R. P., COHEN, I., FALK, R. & KUPERSMITH, J. (1980). Activity-dependent extracellular K^+ fluctuations in canine Purkinje fibres. *Nature, Lond.* **286**, 68–71.

KLINE, R. P., COHEN, I., FALK, R. & KUPERSMITH, J. (1982). Extracellular potassium selective electrode experiments in voltage clamped small canine Purkinje fibers. *Biophys. J.* (in the Press).

KLINE, R. P. & KUPERSMITH, J. (1980). Extracellular K^+ accumulation in canine Purkinje fibers: effects on maximum diastolic potential and action potential duration. *Fedn Proc.* **36**, 996.

KLINE, R. P. & MORAD, M. (1976). Potassium efflux and accumulation in heart muscle. *Biophys. J.* **16**, 367–372.

KLINE, R. P. & MORAD, M. (1978). Potassium efflux in heart muscle during activity: extracellular accumulation and its implications. *J. Physiol.* **280**, 537–558.

KRONHAUS, K., SPEAR, J., KLINE, R. P. & MOORE, E. N. (1978). Sinus node extracellular potassium transients following vagal stimulation. *Nature, Lond.* **275**, 322–324.

KUNZE, D. L. (1977). Rate dependent changes in extracellular potassium in the rabbit atrium. *Circulation Res.* **41** (1), 122–127.

LANGER, G. A. & BRADY, A. J. (1966). Potassium in dog ventricular muscle: kinetic studies of distribution and effects of varying frequency of contraction and potassium concentration of perfusate. *Circulation Res.* **18**, 164–177.

LEE, C. O. & FOZZARD, H. A. (1975). Activities of potassium and sodium ions in rabbit heart muscle. *J. gen. Physiol.* **65**, 695–708.

LUX, H. D. & NEHER, E. (1973). The equilibration time course of (K^+) in cat cortex. *Expl Brain Res.* **17**, 190–205.

MCALLISTER, R. E. & NOBLE, D. (1966). The time and voltage dependence of the slow outward current in cardiac Purkinje fibres. *J. Physiol.* **186**, 632–662.

MACALLISTER, R. E., NOBLE, D. & TSIEN, R. W. (1975). Reconstruction of the electrical activity of cardiac Purkinje fibres. *J. Physiol.* **251**, 1–59.

MIURA, D. S., HOFFMAN, B. & ROSEN, M. R. (1977). The effect of extracellular potassium on the intracellular potassium ion activity and transmembrane potentials of beating canine cardiac Purkinje fibres. *J. gen. Physiol.* **69**, 463–473.

NEHER, E. & LUX, H. D. (1973). Rapid changes of potassium concentration at the outer surface of single neurons during membrane current flow. *J. gen. Physiol.* **61**, 385–399.

NOBLE, S. J. (1976). Potassium accumulation and depletion in frog atrial muscle. *J. Physiol.* **258**, 579–613.

PAPE, L. & KATZMAN, R. (1972). Response of glia in cat sensorimotor cortex to increased extracellular potassium. *Brain Res.* **38**, 71–92.

SPEAR, J., KRONHAUS, K., MOORE, E. N. & KLINE, R. P. (1979). The effect of brief vagal stimulation in the isolated rabbit sinus node. *Circulation Res.* **44**, 75–88.

TRAUTWEIN, W. (1973). Membrane currents in cardiac muscle fibers. *Physiol. Rev.* **53** (4), 793–835.

VASSALLE, M. (1970). Electrogenic suppression of automaticity in sheep and dog Purkinje fibers. *Circulation Res.* **27**, 361–377.

VASSALLE, M. (1977). The relationship among cardiac pacemakers: overdrive suppression. *Circulation Res.* **41**, 269–277.

VEREECKE, J., ISENBERG, G. & CARMELIET, E. (1980). K efflux through inward rectifying K channels in voltage clamped Purkinje fibers. *Pflügers Arch.* **384**, 207–217.

WEIDMANN, S. (1956). Shortening of the cardiac action potential due to a brief injection of KCl following the onset of activity. *J. Physiol.* **132**, 157–163.